Mechanical properties of cubic zinc carboxylate IRMOF-1 metal-organic framework crystals

D. F. Bahr* and J. A. Reid
School of Mechanical and Materials Engineering, Washington State University, Pullman, Washington 99164, USA

W. M. Mook
Department of Chemical Engineering and Materials Science, University of Minnesota, Minneapolis, Minnesota 55455-0000, USA

C. A. Bauer,† R. Stumpf, A. J. Skulan, N. R. Moody, B. A. Simmons, M. M. Shindel, and M. D. Allendorf*
Sandia National Laboratories, Livermore, California 94451-0969, USA
(Received 29 June 2007; published 8 November 2007)

The recently developed class of nanoporous materials known as metal-organic frameworks (MOFs) is generating considerable interest because of their potential in sensing, storage, and chemical separations. In many applications, it is essential to understand their mechanical properties. We report the measurement of the elastic modulus of IRMOF-1 crystals using two different nanoindentation techniques. The reduced modulus from continuous stiffness measurements, calculated from the average single-crystal Young's modulus (E) of 2.7 ± 1.0 GPa, is in good agreement with the value obtained from conventional quasistatic measurements. Permanent deformation without fracture has been observed directly after indentation. For comparison, we performed density functional theory (DFT) calculations of the elastic properties using both the local density approximation (LDA) and the generalized gradient approximation (GGA). The resulting, well-converged DFT value (LDA-GGA average) for E is 21.6 ± 0.3 GPa, with $C_{11}=0.28 \pm 0.01$ GPa, $C_{12}=0.11 \pm 0.01$ GPa, and $C_{44}=0.03 \pm 0.02$ GPa. Correcting the measured modulus for the highly anisotropic elastic behavior predicted by DFT suggests an effective modulus for the (100) face of 7.9 GPa. The DFT prediction is expected to be reliable here. Therefore, the lower measured Young's modulus is most likely due to an interesting behavior during fractureless plastic deformation that occurs in these framework materials. Deformation or buckling in this nanoporous structure likely leads to structural changes at the lowest loads we can apply in the experiment. This appears to be a unique property of MOFs, where the elastic properties of the plastically deformed materials behave differently than those for more traditional nanoporous metals, ceramics, and polymers.

DOI: 10.1103/PhysRevB.76.184106 PACS number(s): 62.25.+g, 62.20.Dc, 61.43.Gt

I. INTRODUCTION

Metal-organic frameworks (MOF), a novel subclass of crystalline coordination polymers, are hybrid inorganic-organic materials whose properties can be tuned by variation of both the metal and organic components.[1] A number of MOFs are nanoporous, exhibiting stable porosity that does not collapse when guest solvent molecules are removed. These materials, such as the isoreticular MOF series created by Eddaoudi *et al.*[2] and the Matérial Institut Lavoisier series of Ferey,[3] include the highest surface-area crystalline compounds known. The combination of crystalline structure and tunable organic ligands enables the rational design of porosity at the nanoscale. As a result, there is growing interest in developing MOFs tailored for applications such as gas storage,[4] chemical separations,[5] catalysis,[6–8] drug delivery,[9] and sensors.[10,11]

In many of these applications, knowledge of the mechanical properties is important for designing MOFs with optimal properties. Specifically, the interface strength between a MOF layer and a substrate is a function of the elastic energy cost induced by a lattice or thermal expansion mismatch between the MOF and substrate. Recently, several studies of the cubic zinc carboxylate IRMOF-1 [formula unit $Zn_4O(1,4\text{-benzenedicarboxylate})_3$, formerly designated MOF-5] appeared, in which density functional theory (DFT) was used to predict the single-crystal elastic constants (C_1, C_{12}, C_{44}, see Table I). Mattesini *et al.* were the first to report these, employing the local density approximation (LDA) in a local orbital calculation (SIESTA).[12] Their results suggest that IRMOF-1 is a soft and ductile material, having a Young's modulus comparable to that of oak wood. Samanta *et al.*[13] used DFT-LDA with the more accurate projector augmented-wave (PAW) method in the VASP code, obtaining rather different results.[13] In particular, they found that the shear modulus C_{44} is small, indicating that this MOF is close to being structurally unstable. Finally, Zhou and Yildirim[14] reported the calculated elastic and the calculated and measured vibrational properties of IRMOF-1. Again, the calculations are performed within DFT-LDA with ultrasoft pseudopotentials.[14] They confirmed the small C_{44} shear modulus of Samanta *et al.*[13] Their measured and calculated neutron inelastic scattering results largely agree, giving support to the reliability of the calculated elastic properties. The predicted lattice parameters are all close to, but slightly below, the experimental value obtained by neutron diffraction from deuterated IRMOF-1 at 3.5 K (25.91 Å).[15] This is typical for LDA calculations.

To provide data for comparison with theory, we performed nanoindentation measurements on IRMOF-1 single crystals. Load versus displacement curves obtained from these measurements yield the stiffness, reduced modulus (which can be related to the Young's modulus), and hardness of the material. Two different nanoindentation techniques were used: a continuous stiffness measurement (CSM) tech-

TABLE I. Summary of DFT predictions of IRMOF-1 elastic constants.

Source	DFT	Core	a_{lat} (Å)	Density (g/cm^3)	B_0 (GPa)	C_{11} (GPa)	C_{12} (GPa)	C_{44} (GPa)	E (GPa)	ν
This work	GGA	PAW	26.04	0.580	16.3	27.8	10.6	3.6	21.9	0.28
This work	LDA	PAW	25.59	0.611	17.6	28.5	12.1	1.7	21.3	0.30
This work	Average	PAW	25.8±0.6	0.60±0.03	17.0±0.6	28.2±0.4	11.4±0.8	2.7±1	21.6	0.29
Mattesini *et al.*[a]	LDA	Norm Cons.	25.89	0.589	17.0	21.5	14.8	7.5	9.4	0.41
Samanta *et al.*[b]	LDA	PAW	25.64	0.607	18.5	29.2	13.1	1.4	21.1	0.31
Zhou and Yildirim[c]	LDA	USP	25.58	0.611	18.2	29.4	12.6	1.2	21.9	0.30

[a]Reference 12.
[b]Reference 13.
[c]Reference 14.

nique and quasistatic indentation employing the Oliver-Pharr analysis method.[16] These techniques are found to yield consistent results in over 30 measurements on five different crystals. The measurements provide a mean value of the Young's modulus for comparison with DFT calculations.

Our DFT calculations are well converged and we use both LDA and the generalized gradient approximation (GGA). Comparing these two approximations makes sense because this provides a fundamental error margin for theory. Often, the mean between LDA and GGA gives the most reliable results, exemplified by the fact that experimental lattice constants and bulk moduli are quite often bracketed by the LDA and GGA values. To eliminate further numerical issues, we derive the bulk modulus (B_0) and elastic constants (C_{11}, C_{12}, and C_{44}) from the calculated stress tensor at a single, small strain. The combined theory and indentation results, coupled with the previously reported DFT calculations, enable comparison of predicted mechanical properties with measurements. As will be seen, a substantial discrepancy is observed, the reasons for which are discussed below.

II. EXPERIMENTAL METHODS

IRMOF-1 single crystals were prepared using a method similar to that reported by Eddaoudi *et al.*[2] Briefly, 67 mg of 1,4-benzenedicarboxylic acid (99+%, ACROS Organics, Belgium) and 357 mg of $Zn(NO_3)_2 \cdot 6H_2O$ (Fluka; ⩾99%) were dissolved in 10 ml of N,N'-diethylformamide (DEF; TCI America) in a Pyrex bottle and sealed. This was heated for 16 h at 105 °C, after which the solvent was decanted. The crystals were washed twice with 10 ml of fresh N,N'-dimethylformamide (DMF; Alfa Aesar). The solvents were exchanged with 10 ml of chloroform three times, allowing the crystals to soak for 24 h with each exchange. The last solvent wash was decanted, leaving crystals slightly wet with chloroform. A portion of the crystals was stored in chloroform until testing, at which point they were mounted for nanoindentation and allowed to dry in ambient environment. Another portion was dried from chloroform under slowly decreasing pressure to a final pressure of 20 mTorr and periodically purged with dry nitrogen, as we noted sensitivity of the evacuated crystals to prolonged exposure to ambient air and rapid evacuation of the solvent. These crystals were dried for approximately 30 min and kept under dry nitrogen until ready for measurement.

Two different nanoindentation techniques[16] were used and found to yield consistent results. The first is the CSM technique performed on an MTS Nano Indenter XP (MTS Corp., Eden Prairie, MN). Here, the stiffness of the IRMOF-1 single crystal is measured throughout the displacement-controlled indentation process by the superposition of a 2 nm sinusoidal displacement on the tip at a frequency of 45 Hz. By evaluating stiffness in this manner, both hardness and reduced modulus can be determined continuously if the tip-sample contact area as a function of displacement is known. The area function of the Berkovich tip used here was determined by indenting a reference material (in this case, fused quartz) with known elastic properties. All tests using the CSM technique were conducted on crystals at room temperature and at ambient relative humidity within 1 h of the drying process described above. During indentation, they were translucent but then deteriorated within a few hours to an opaque appearance.

A second set of tests was performed on the crystals using quasistatic indentation employing the Oliver-Pharr analysis method.[16] These samples were stored in chloroform prior to testing. After removal from the chloroform, samples were adhered to a sample holder using cyanoacrylic adhesive. The habit planes of a given IRMOF crystal were oriented such that an external face would align perpendicular to the indenter direction. Using a Hysitron (Minneapolis, MN) Triboscope coupled with a Park Scientific (Santa Barbara, CA) Autoprobe CP scanning probe microscope, IRMOF crystals were imaged using a constant force imagining technique with a diamond Berkovich indenter tip. After selecting a relatively flat region of the crystal, indentations were made using a quasistatic indentation at loading and unloading rates of approximately 10 μN/s. The stepped nature of the habit planes of these materials is shown in Fig. 1, as well as the resulting impression formed from a quasistatic indentation. There are large scale (tens of nanometers high) steps and pits on the surface. However, relatively flat regions, on the order of 1–5 μm across, can be identified using scanning probe microscopy and the indentations were carried out in these areas. Selecting these flat regions of the crystals for testing

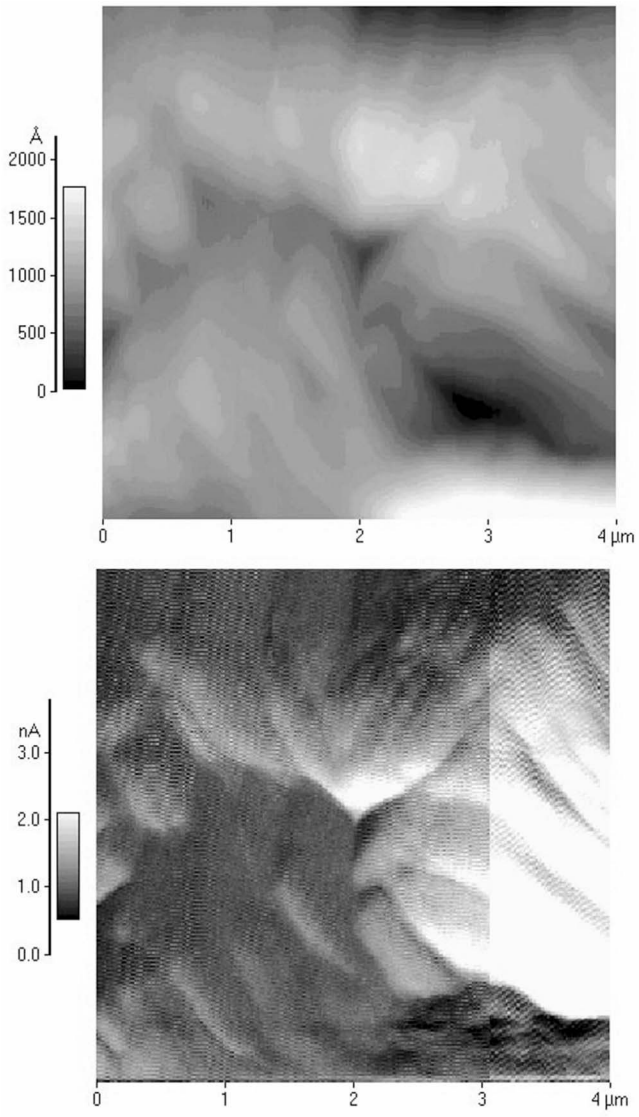

FIG. 1. Scanning probe microscopy height (top) and deflection (bottom) images of a residual impression on the habit planes of the IRMOF-1 crystals. Step heights of 10–100 nm separated by hundreds of nanometers were present on the surface, along with larger steps (1–10 μm) separated laterally by tens of micrometers.

greatly enhanced the reproducibility of the nanoindentation experiments. An analysis of the unloading slope was used to determine the modulus and hardness of the samples. Five different crystals were selected for testing. Most tests were carried out within 30 min of mounting the samples and exposure to ambient environmental conditions. One set of samples was retested after 4 h and 6 days of exposure to ambient atmospheric conditions.

III. THEORETICAL METHODS

We performed DFT calculations using the VASP code[17,18] and applied GGA (Ref. 19) and LDA (Ref. 20) to obtain an estimate of the fundamental reliability of our results. To accurately represent the atomic cores, we use the PAW technique.[21] Electronic wave functions are represented by plane waves up to 400 eV, with tests up to 520 eV. Bulk calculations were performed in the rhombohedral, 106-atom, primitive cell, and the cubic, 424-atom, conventional cell. K-space sampling is sufficient with the Γ point only as tests with up to four special k points show. In all calculations, atomic positions were relaxed with residual forces below 3 meV/Å. The typical procedure used to obtain the bulk modulus and elastic constants is to calculate a range of energies as a function of applied strain (or lattice constant), which are then fitted to a Birch-Murnaghan[22] or a similar equation of state.[23] This approach is unreliable here, because the total energy as a function of strain is not smooth enough, especially within 1% of the equilibrium lattice constant. To eliminate these numerical issues, we derive the bulk modulus (B_0) and elastic constants (C_{11}, C_{12}, and C_{44}) from the change of the directly calculated stress tensor at a single, small strain of 0.5%.

IV. RESULTS

A. Density functional theory calculations

Our LDA results are fairly close to those of Zhou and Yildirim[14] and Samanta *et al.*[13] (see Table I). This confirms the small value for the shear modulus C_{44}, which indicates a near instability of the IRMOF-1 structure. As usual, GGA predicts a larger lattice constant, resulting in mostly softer elastic constants. The exception is C_{44}, which is double that predicted by LDA. Table I also provides the LDA-GGA averages with a confidence interval based on the LDA-GGA difference and the numerical uncertainty. We obtain the Young's modulus E and Poisson's ratio ν from Eqs. (1) and (2) for cubic single crystals:

$$E = \frac{(C_{11} + 2C_{12})(C_{11} - C_{12})}{C_{11} + C_{12}}, \tag{1}$$

$$\nu = \frac{C_{12}}{(C_{11} + C_{12})}. \tag{2}$$

These equations yield 21.6±0.3 GPa for E and 0.28±0.01 for ν based on the average C_{11} and C_{12} values in Table I. The modulus in a given orientation can be determined from[24]

$$\frac{1}{E} = S_{11} - 2\left((S_{11} - S_{12}) - \frac{1}{2}S_{44}\right)(l^2m^2 + m^2n^2 + l^2n^2), \tag{3}$$

where S is the compliance matrix (the inverse matrix described by the stiffness matrix in Table I), and l, m, n are the direction cosines between the face of interest and the axis. For this material, we expect a range of moduli in different directions from 21.6 GPa in (100) to 7.5 GPa in (111).

B. Nanoindentation measurements

The residual impressions from the quasistatic indentations to contact depths of 200 nm are on the order of the size of the small terraces on the habit plane. The modulus and hardness as a function of depth obtained from the CSM measurements, shown in Fig. 2, go to larger contact depths and therefore sample many steps. The hardness and modulus values at

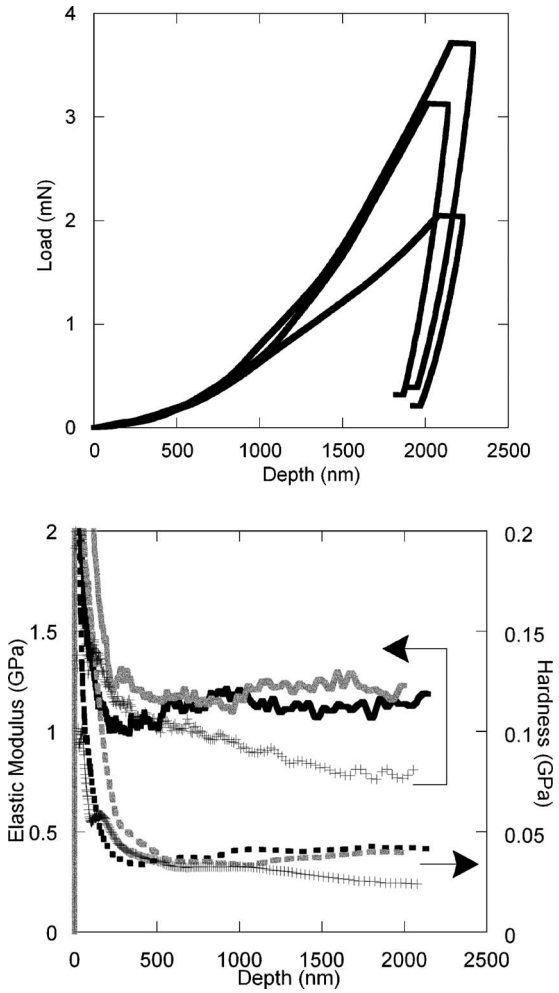

FIG. 2. Indentation of IRMOF-1 single crystals using CSM showing (top) load-displacement relation for three indents and (bottom) the elastic modulus (solid lines) and hardness (dotted lines) relations for the indents.

depths less than 500 nm could be due to surface roughness effects that lead to inaccuracies in measurements,[25] while the values at greater depths are characteristic of this IRMOF-1 structure. Similar data have been collected from the quasistatic tests. The initial change in modulus and hardness in the quasistatic tests occurs over the first 100 nm of depth. When relatively flat areas are selected, the modulus and hardness are essentially constant beyond 100 nm. The modulus measured by the quasistatic test (Fig. 3) shows a slightly higher value than that of the CSM tests (Fig. 2).

The mean reduced modulus obtained from 32 CSM tests in a crystal within 1 h of mounting is 2.7±1.0 GPa. The reduced modulus E_b (shown in Fig. 3) is defined as

$$\frac{1}{E_r} = \frac{1-\nu_i^2}{E_i} + \frac{1-\nu_s^2}{E_s}, \tag{4}$$

where E and ν are the Young's modulus and Poisson's ratio, respectively, and the subscripts i and s refer to indenter and sample, respectively.

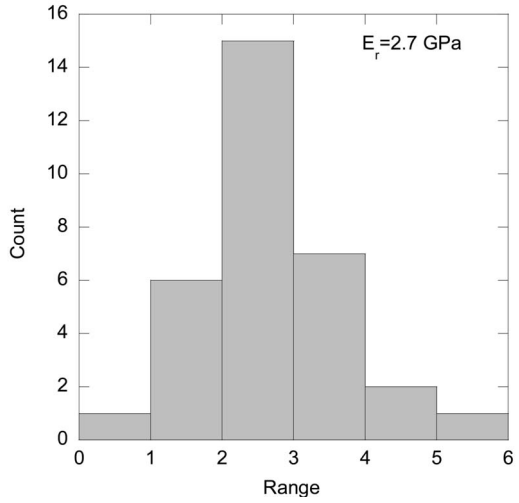

FIG. 3. Histogram of reduced elastic modulus of 32 quasistatic indentations in IRMOF-1 at depths between 150 and 500 nm using the Hysitron Triboscope. Both the modulus and hardness exhibit a normal distribution in values over this range of sampling volumes.

For the conventional (quasistatic) indentation technique, diamond is selected for the indenter tip with E_i=1149 GPa and ν_i=0.07. If one assumes our theoretical Poisson's ratio ν_s of IRMOF-1 of 0.28, the Young's modulus E_s obtained from the quasistatic measurements is 2.5±1.0 GPa. The choice of ν_s is not critical here. A change in ν_s of 10% leads to at most 3% change in E_s. The average hardness from the quasistatic measurements is 58 MPa, with a standard deviation of 26 MPa. This is 20% higher than the values measured by CSM. Typical quasistatic indentation tests are shown in Fig. 4, with two notable features. First, there is significant creep at the maximum load; this is also evident in the CSM tests. Second, there is adhesion between the tip and sample upon complete unloading, which manifests as a "pull off load" of approximately 6 μN in this particular experiment. Scanning probe imaging was carried out after typical indentations (Fig. 1) and revealed no fracture around these indentations, sug-

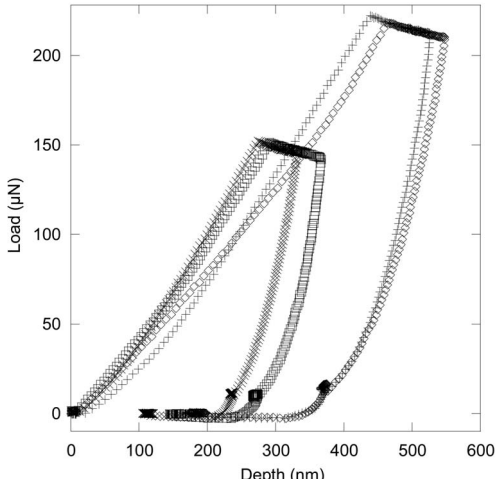

FIG. 4. Typical quasistatic indentations of IRMOF-1 showing significant creep during a hold at maximum load and tip-sample adhesion (approximately 6 μN) upon retraction of the tip.

gesting that the measured properties reported in this paper are not influenced by indentation-induced fracture. This is a unique observation, indicating that these materials deform under contact loading plastically, either by plastic flow or densification, rather than microscopic fracture. Plastic deformation is present at applied loads of 17 μN (which corresponds to an applied pressure of approximately 20 MPa) from the shallowest indentations performed in this study.

V. DISCUSSION

The Young's modulus obtained from the CSM nanoindentation measurements (2.7 ± 1.0 GPa) is in significant disagreement with the average value of 21.6 ± 0.3 GPa from DFT. However, as the IRMOF-1 is highly anisotropic in its elastic response, this must be accounted for when interpreting the experimental data. Based on the work of Vlassak and Nix,[26] it is possible to account for the elastic anisotropy using a correction factor to the indentation modulus. The anisotropy factor (E_{100}/E_{111}) is 2.88 for this material, and using the procedures described in Ref. 26, the correction factor to the modulus would be 0.34, such that the measured modulus is likely 2.94 times lower than the modulus in the (100) direction. With this correction factor, the estimated modulus from the indentation measurements is 7.9 GPa for (100) IRMOF-1. Therefore, the measured modulus is approximately one-third of the calculated value.

Three aspects of the mechanical testing of the IRMOF-1 samples and the observed depth dependence of material properties may partially account for this difference: (1) surface roughness in the as-prepared samples, (2) air exposure during measurement, and (3) plastic deformation impacting elastic properties. As the IRMOF-1 crystals were tested in the as-grown condition, faceting and terraces on the growth surface are unavoidable. This leads to a surface roughness effect on the measured properties from contact, which can be minimized by selecting regions of surfaces that are free of macroscopic structural features such as pits. The facets themselves are sloped and not completely perpendicular to the indentation direction. These imperfections lead to scatter and systematic deviations in measured modulus and hardness. CSM measurements at optically selected regions can avoid the macroscopic (tens of micrometers) surface defects. The scanning probe methods avoid defects at the 0.1 μm level. Surface roughness leads to underestimation of modulus and hardness when using area functions that are calibrated from nominally flat materials. Thus, the results presented here may underestimate the actual values. An estimate can be made by comparing CSM measurements at rougher and quasistatic measurements at flatter regions. The flatter regions lead to about 20% higher hardness and 100% higher modulus values. Based on these tests, we estimate that the modulus measured on a perfectly flat crystal would be at most 5 GPa higher than the estimated value of 7.9 GPa, which does not fully account for the difference between the DFT calculations and the measured value.

A second issue is that the IRMOF-1 crystals do alter their behavior with time during testing. Upon removal from chloroform, the samples are optically clear. The chloroform evaporates over the span of 1 min, with the crystals remaining optically clear. However, after approximately 1 h of exposure to ambient atmosphere and mechanical testing, the samples become opaque, with a whitish color. This transition occurs gradually. Two repeat measurements using quasistatic indentation made after 4 h and after 6 days of exposure to atmosphere exhibit an elastic modulus decrease of approximately 20% compared with measurements made within 1 h on the same specimen. If interactions between the atmosphere and the crystal are responsible for these changes in opacity, they may also impact the mechanical properties. Water vapor is known to degrade IRMOFs.[27,28] Similarly, if there is residual solvent or other substances within the MOF pores that only slowly evaporate, this could impact mechanical properties. The modulus appears to decrease slowly with time, so it is possible that some of the difference between the DFT calculations and measured elastic modulus is due to the difficulty of determining the properties of these materials in a pristine condition. However, for the limited measurement times used here (4 h), the elastic properties are relatively constant after exposure to ambient conditions. In addition, crystals stored by two methods (in chloroform and evacuated and backfilled with nitrogen, as described in Sec. II) are found to give similar results, suggesting that the presence of residual solvent in the lattice does not affect the elastic properties.

The third, and probably most significant effect, is the inherent assumption in nanoindentation testing that the elastic properties are the same upon loading and unloading. Extracting properties from nanoindentation data traditionally relies on the assumption that the loading behavior is both elastic and plastic, while the unloading behavior is commonly assumed to be a result of elastic deformation. At our lowest load indentations in this material (17 μN), there was permanent deformation after testing. Because of the extensive open structure in these crystals, the structure after permanent deformation may not be identical to the initial structure. An analogy would be the deformation of a buckled structure. It is well known that macroscopic beam structures that are buckled are more compliant than their initial state. Similarly, recent nanoindentation testing of vertically aligned carbon nanotube turf structures[29,30] has shown that a buckled nanostructure can be orders of magnitude more compliant than in tension and, in fact, continues to exhibit a lower effective modulus upon continued compressive loading. The possible similarities with the IRMOF-1 structure suggest that the discrepancies between the theory and experiment could be a result of the inability to probe only elastic deformation in these structures, and that their deformation behavior is likely significantly different than that of other nanoporous materials, which exhibit an increase in modulus with densification, such as gold.[31,32] The hardness of the crystals was low enough that we were unable to separate any purely elastic load-displacement curves during nanoindentation. To reach lower strains, the conventional method in indentation is to increase the included contact angle of the indenter. For example, using a large spherical tip at low penetration depths will provide an extremely low effective strain.[33] However, due to the surface roughness of these materials, increasing the indenter tip radius is not a viable option, as the surface

roughness will then dominate the initial contact behavior. The possible change in structure responsible for the permanent deformation could be viewed similarly to a phase transition in solids, where the unloading portion of the indentation is altered by the phase transformation under the indentation region.[36] Further work on characterizing this local structure could be enlightening but is beyond the scope of the current study.

In general, the DFT methods used here perform well with regard to predicting the elastic and vibrational properties of solids and molecules. We are unaware of any significant failures, certainly not close to the factor of 3 at issue here. DFT has been applied to surfaces and open structures, as well as novel materials such as nanocarbon structures.[34] Elastic properties are also usually described well, including materials at very high pressures within the earth's mantle,[35] and often scale with the lattice constant. Thus, the fact that our calculations correctly predict the IRMOF-1 lattice constant is significant and we therefore ascribe differences between theory and experiments primarily to the three experimental issues: surface roughness, atmospheric interactions, and plastic deformations.

VI. CONCLUSIONS

The elastic and plastic response of the metal-organic framework IRMOF-1 has been measured via nanoindentation and the results have been compared to elastic constants predicted by DFT. The Young's modulus measured via CSM nanoindentation, approximately 2.7 GPa, is about an order of magnitude lower than that predicted by DFT. After accounting for the anisotropic elastic behavior, the measured value is still a factor of 3 lower than the predicted values. Surface roughness, which prevents measurements at small indentation from staying within the elastic limit of the IRMOF-1 crystal, is a factor in lowering the measured moduli. The sensitivity of these materials to atmospheric conditions may also be partially responsible for the differences between these values. Surprisingly, plasticity without fracture is observed during contact loading of these materials even at small (<100 nm) indentation amplitudes. This may be the most significant contribution to the lowering of the measured moduli and indicates that the differences between experimental and theoretical behaviors cannot be ascribed to fracture processes in these macroscopically brittle materials. These results suggest that postyield elastic properties, applied stresses, and subsequent deformation will need to be considered for applications involving these materials and they will likely require inert atmospheres and low applied stresses to maintain their structural integrity.

ACKNOWLEDGMENTS

We gratefully acknowledge Jonathan Zimmerman for helpful discussions. This project was funded by the Laboratory Directed Research and Development Program of Sandia National Laboratories.

*Corresponding authors.
†Present address: Department of Chemistry and Biochemistry, Georgia Institute of Technology, Atlanta, GA 30332-0400.

[1] S. L. James, Chem. Soc. Rev. **32**, 276 (2003).
[2] M. Eddaoudi, J. Kim, N. Rosi, D. Vodak, J. Wachter, M. O'Keefe, and O. M. Yaghi, Science **295**, 469 (2002).
[3] G. Ferey, Chem. Mater. **13**, 3084 (2001).
[4] J. L. C. Rowsell and O. M. Yaghi, Angew. Chem., Int. Ed. **44**, 4670 (2005).
[5] R. Q. Snurr, J. T. Hupp, and S. T. Nguyen, AIChE J. **50**, 1090 (2004).
[6] S. Hermes, M.-K. Schroter, R. Schmid, L. Khodeir, M. Muhler, A. Tissler, R. W. Fischer, and R. A. Fischer, Angew. Chem., Int. Ed. **44**, 6237 (2005).
[7] P. Mahata, G. Madras, and S. Natarajan, J. Phys. Chem. B **110**, 13759 (2006).
[8] C.-D. Wu, A. Hu, L. Zhang, and W. Lin, J. Am. Chem. Soc. **127**, 8940 (2005).
[9] P. Horcajada, C. Serre, M. Vallet-Regi, M. Sebban, F. Taulelle, and G. Ferey, Angew. Chem., Int. Ed. **45**, 5974 (2006).
[10] C. A. Bauer, T. V. Timofeeva, T. B. Settersten, B. D. Patterson, V. H. Liu, B. A. Simmons, and M. D. Allendorf, J. Am. Chem. Soc. **129**, 7136 (2007).
[11] Z. Ni, J. P. Jerrell, K. R. Cadwallader, and R. I. Masel, Anal. Chem. **79**, 1290 (2007).
[12] M. Mattesini, J. M. Soler, and F. Yndurain, Phys. Rev. B **73**, 094111 (2006).
[13] A. Samanta, T. Furuta, and J. Li, J. Chem. Phys. **125**, 084714 (2006).
[14] W. Zhou and T. Yildirim, Phys. Rev. B **74**, 180301(R) (2006).
[15] T. Yildirim and M. R. Hartman, Phys. Rev. Lett. **95**, 215504 (2005).
[16] W. C. Oliver and G. M. Pharr, J. Mater. Res. **19**, 3 (2004).
[17] G. Kresse and J. Furthmuller, Comput. Mater. Sci. **6**, 15 (1996).
[18] G. Kresse and J. Furthmuller, Phys. Rev. B **54**, 11169 (1996).
[19] Y. Wang and J. P. Perdew, Phys. Rev. B **44**, 13298 (1991).
[20] J. P. Perdew and A. Zunger, Phys. Rev. B **23**, 5048 (1981).
[21] P. E. Blochl, Phys. Rev. B **50**, 17953 (1994).
[22] F. D. Murnaghan, Proc. Natl. Acad. Sci. U.S.A. **30**, 244 (1944).
[23] P. Soderlind, O. Eriksson, J. M. Wills, and A. M. Boring, Phys. Rev. B **48**, 5844 (1993).
[24] G. E. Dieter, *Mechanical Metallurgy* (McGraw-Hill, New York, 1986).
[25] M. S. Bobji and S. K. Biswas, J. Mater. Res. **14**, 2259 (1999).
[26] J. Vlassak and W. D. Nix, J. Mech. Phys. Solids **42**, 1223 (1994).
[27] J. A. Greathouse and M. D. Allendorf, J. Am. Chem. Soc. **128**, 10678 (2006).
[28] L. Huang, H. Wang, J. Chen, Z. Wang, J. Sun, D. Zhao, and Y. Yan, Microporous Mesoporous Mater. **58**, 105 (2003).
[29] C. M. McCarter, R. F. Richards, S. Mesarovic, C. D. Richards, D. F. Bahr, D. McClain, and J. Jiao, J. Mater. Sci. **41**, 7872 (2006).
[30] S. D. Mesarovic, C. M. McCarter, D. F. Bahr, H. Radhakrishnan,

R. F. Richards, C. D. Richards, D. McClain, and J. Jiao, Scr. Mater. **56**, 157 (2007).
[31] A. M. Hodge, J. Biener, J. R. Hayes, P. M. Bythrow, C. A. Volkert, and A. V. Hamza, Acta Mater. **55**, 1343 (2007).
[32] C. A. Volkert, E. T. Lilleodden, D. Kramer, and J. Weissmüller, Appl. Phys. Lett. **89**, 061920 (2006).
[33] D. Tabor, *The Hardness of Metals* (Oxford, Oxford, 1951).
[34] J. Bernholc, D. Brenner, M. B. Nardelli, V. Meunier, and C. Roland, Annu. Rev. Mater. Res. **32**, 347 (2002).
[35] B. B. Karki, L. Stixrude, and R. M. Wentzcovitch, Rev. Geophys. **39**, 507 (2001).
[36] V. Domnich, Y. Gogotsi, and S. Dub, Appl. Phys. Lett. **76**, 2214 (2000).